# $L_2$ sensitivity paper update

J. Huston
Michigan State University
for L2 sensitivity authors

MSUHEP-23-XX, SMU-HEP-23-XX,DESY-23-XX...

# Sensitivities of fits of parton distributions to experimental constraints

Xiaoxian Jing,[1] Amanda Cooper-Sarkar,[2] Aurore Courtoy,[3] Thomas Cridge,[4] Francesco Giuli,[5] Lucian Harland-Lang,[6] T. J. Hobbs,[7] Joey Huston,[8] Pavel Nadolsky,[1,*] Keping Xie,[9] Robert S. Thorne,[6] and C.-P. Yuan[8]

[1] *Department of Physics, Southern Methodist University, Dallas, TX 75275-0181, USA*
[2] *Department of Physics, University of Oxford, Oxford, OX1 3RH, UK*
[3] *Instituto de Física, Universidad Nacional Autónoma de México, Apartado Postal 20-364, 01000 Ciudad de México, Mexico*
[4] *Deutsches Elektronen-Synchrotron DESY, Notkestr. 85, Hamburg, 22607, Germany*
[5] *CERN, CH-1211 Geneva, Switzerland*
[6] *Department of Physics and Astronomy, University College, London, WC1E 6BT, UK*
[7] *High Energy Physics Division, Argonne National Laboratory, Argonne, IL 60439, USA*
[8] *Department of Physics and Astronomy, Michigan State University, East Lansing, MI 48824, USA*
[9] *Pittsburgh Particle Physics, Astrophysics and Cosmology Center, Department of Physics and Astronomy, University of Pittsburgh, Pittsburgh, PA 15260, USA*

(Dated: April 28, 2023)

**...in progress**

# Prelude: uncertainties

- PDF uncertainties depend first on the experimental uncertainties of the data
- Data from two measurements, or even from within the same measurement, can both be very precise, but the result of adding both to the PDF fit can be an increase in the PDF uncertainty (or more likely) a smaller decrease in uncertainty than expected) if the data are in tension with each other
- The resultant PDF uncertainty relies on the definition of a tolerance, i.e. what is a significant increase from the global minimum $\chi^2$, i.e. PDF uncertainty can be adjusted by changing the tolerance
- $\Delta\chi^2=1$ is not applicable for ~4000 data points from different experiments
- NB: CT (Tier 2) and MSHT (dynamic tolerance) have introduced criteria to restrict the pull of data sets that disagree with global fit

# What is the $L_2$ sensitivity?

- For data to influence the PDF fit in a particular region of x and $Q^2$, two conditions must be met
  - the parton-level dynamics must depend on a particular PDF (say that of the gluon), as manifested in a statistical correlation
  - the data must have sufficient resolving power to contribute to the PDF likelihood analysis
- The $L_2$ sensitivity incorporates both of these features
- The $L_2$ sensitivity is a way of viewing the pulls of all of the experiments used in a global PDF fit, for a particular parton flavor, as a function of a kinematic variable, such as parton x
  - or, when plotted for a PDF luminosity, as a function of the mass
- The fit value for a particular PDF(x,Q) is determined by the sum of these pulls

# What is the $L_2$ sensitivity…continued?

- The $L_2$ sensitivity provides a visualization of what is happening inside the PDF fit
- It can be considered as a faster version of Lagrange Multiplier scans (but dependent on the Gaussian approximation)
- The $L_2$ sensitivity streamlines comparisons among independent analyses, using the log-likelihood ($\chi^2$) values for the fitted experiments and the error PDFs
- Both the $L_2$ and LM methods explore the parametric dependence of the $\chi^2$ function in the vicinity of the global minimum
- The $L_2$ sensitivity has been used internally by CT (in CT18), by the PDF4LHC21 benchmarking group (to determine which data sets should be in the reduced PDF fit used for benchmarking), and now by CT, MSHT and ATLASpdf in this upcoming paper

# Error PDFs

- ATLAS, CT and MSHT groups adopt the Hessian format for their PDF error sets
- D error PDFs are used to determine the PDF uncertainty (assuming the probability distribution is approximately Gaussian)
- Consider an expansion of a function X of the parameters R in the vicinity of the global $\chi^2$ minimum $X_o$

$$X(\vec{R}) = X_0 + \sum_{i=1}^{D} \frac{\partial X}{\partial R_i}\bigg|_{\vec{R}=\vec{0}} R_i + \frac{1}{2}\sum_{i,j=1}^{D} \frac{\partial^2 X}{\partial R_i \partial R_j}\bigg|_{\vec{R}=\vec{0}} R_i R_j + \dots .$$

$$\frac{\partial X}{\partial R_i}\bigg|_{\vec{R}=\vec{0}} \approx \frac{X_{+i} - X_{-i}}{2}.$$

use symmetrized form for first order derivative

$$\Delta^{\mathrm{H}} X = \left|\vec{\nabla} X\right| = \frac{1}{2}\sqrt{\sum_{i=1}^{D} \left[X_{+i} - X_{-i}\right]^2}.$$

define 68% CL hypersphere

$$C^{\mathrm{H}}(X,Y) = \frac{1}{4\Delta^{\mathrm{H}} X \Delta^{\mathrm{H}} Y} \sum_{i=1}^{D} (X_{+i} - X_{-i})(Y_{+i} - Y_{-i})$$

define correlation between 2 variables X and Y

# $L_2$ sensitivity

$$S^{\mathrm{H}}_{f,L2}(E) \equiv \frac{\vec{\nabla}\chi^2_E \cdot \vec{\nabla} f}{\Delta^{\mathrm{H}} f} = \left(\Delta^{\mathrm{H}}\chi^2_E\right)\ C^{\mathrm{H}}(f, \chi^2_E)$$

$2^{nd}$ Lagrangian technique

- $C^H$ represents the cosine of the correlation angle between PDF flavor f (or any defined quantity) and experimental $\chi^2$

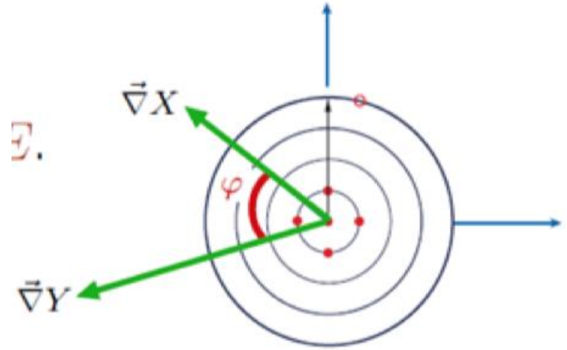


The importance of an experiment for a particular PDF depends not only on the correlation of the cross section with that PDF, but the degree to which the cross section can determine that PDF.

- Can also be defined for the MC PDF approach

# Estimated $\chi^2$ pulls from experiments

## ($L_2$ sensitivity, T. Hobbs et al., arXiv:1904.00222, v. 2)

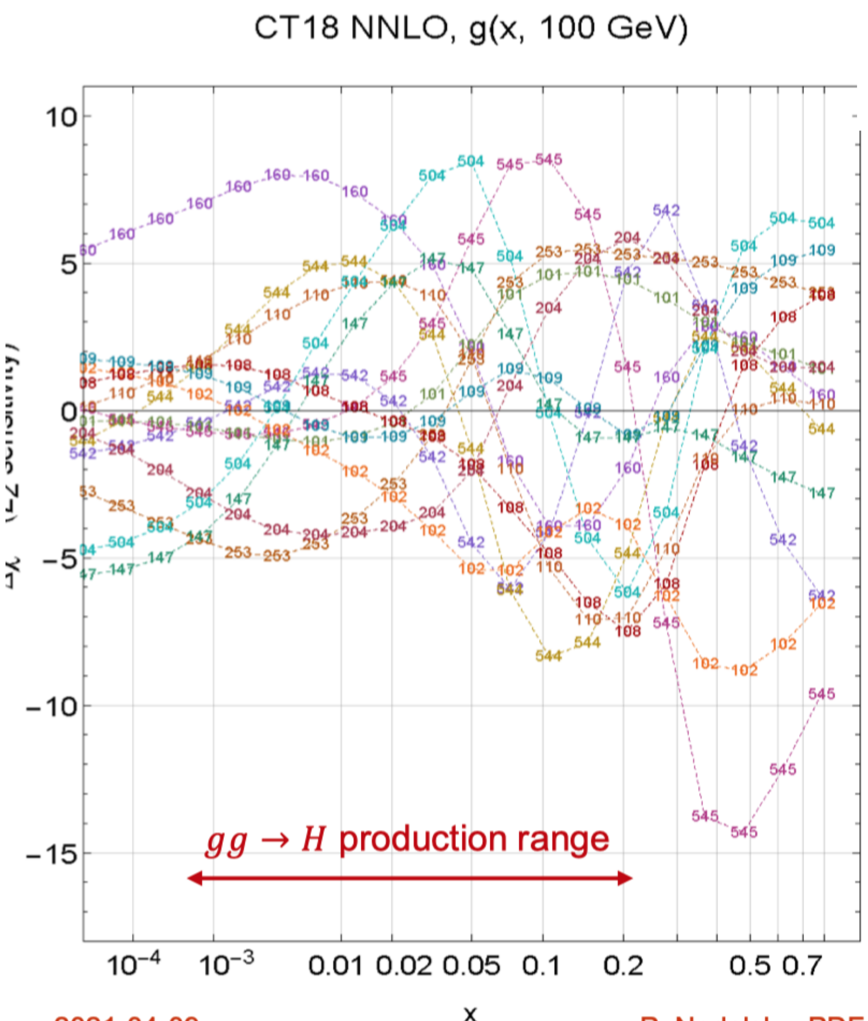


Plots of $L_2$ sensitivities to various PDFs:

CT18 NNLO, gluon at Q=100 GeV

**15 core-minutes**

Most sensitive experiments

- 253 ATL8ZpTbT
- 542 CMS7jtR7y6T
- 544 ATL7jtR6uT
- 545 CMS8jtR7T
- 160 HERAIpII
- 101 BcdF2pCor
- 102 BcdF2dCor
- 108 cdhswf2
- 109 cdhswf3
- 110 ccfrf2.mi
- 147 Hn1X0c
- 204 e866ppxf
- 504 cdf2jtCor2

Experiments with large $\Delta\chi^2 > 0$ $[\Delta\chi^2 < 0]$ pull $g(x, Q)$ in the negative [positive] direction at the shown $x$

# Estimated $\chi^2$ pulls from experiments

## ($L_2$ sensitivity, T. Hobbs et al., arXiv:1904.00222, v. 2)

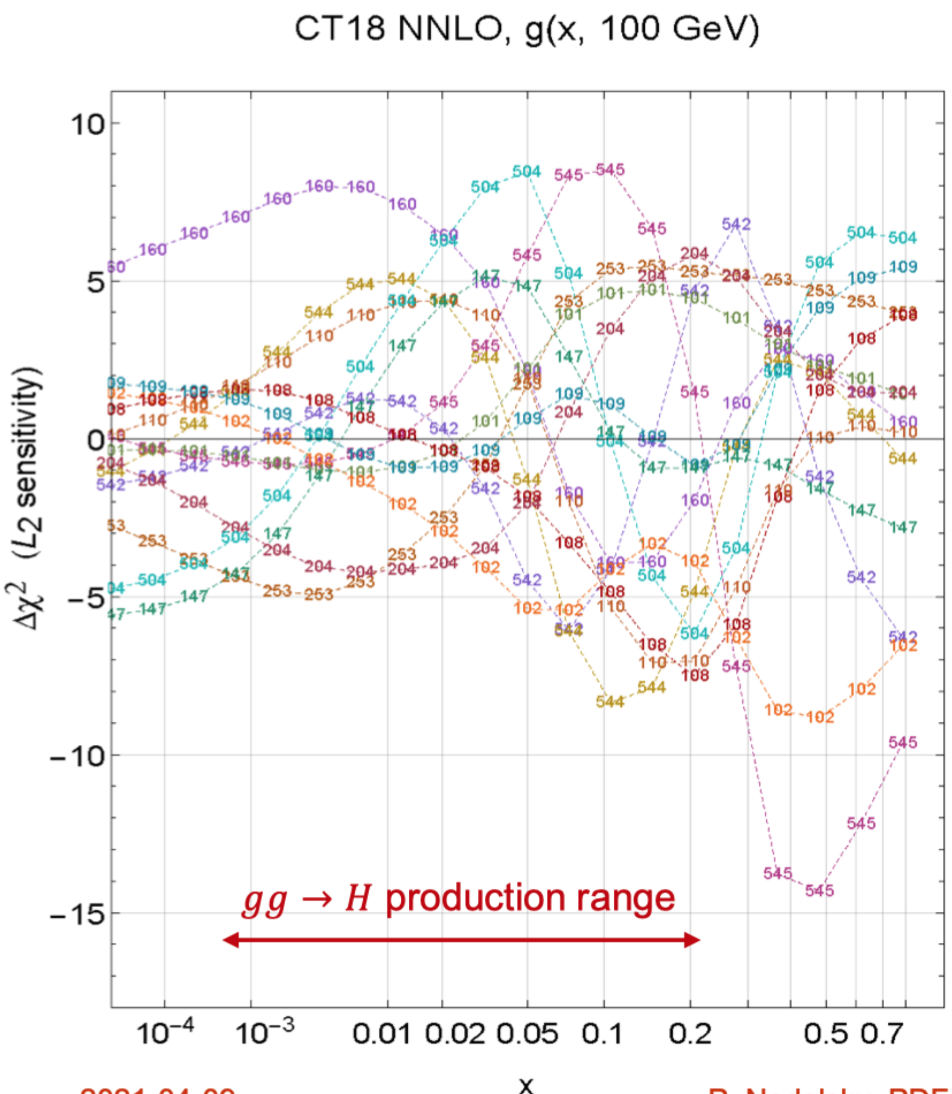


Plots of $L_2$ sensitivities to various PDFs:
https://ct.hepforge.org/PDFs/ct18/figures/L2Sensitivity/

CT18 NNLO, gluon at Q=100 GeV

**15 core-minutes**

Note opposite pulls (tensions) in some x ranges between HERA I+II DIS (ID=160); CDF (504), ATLAS 7 (544), CMS 7 (542), CMS 8 jet (545) production; E866pp DY (204); ATLAS 8 Z pT (253) production; BCDMS and CDHSW DIS show only 6 most important experiments

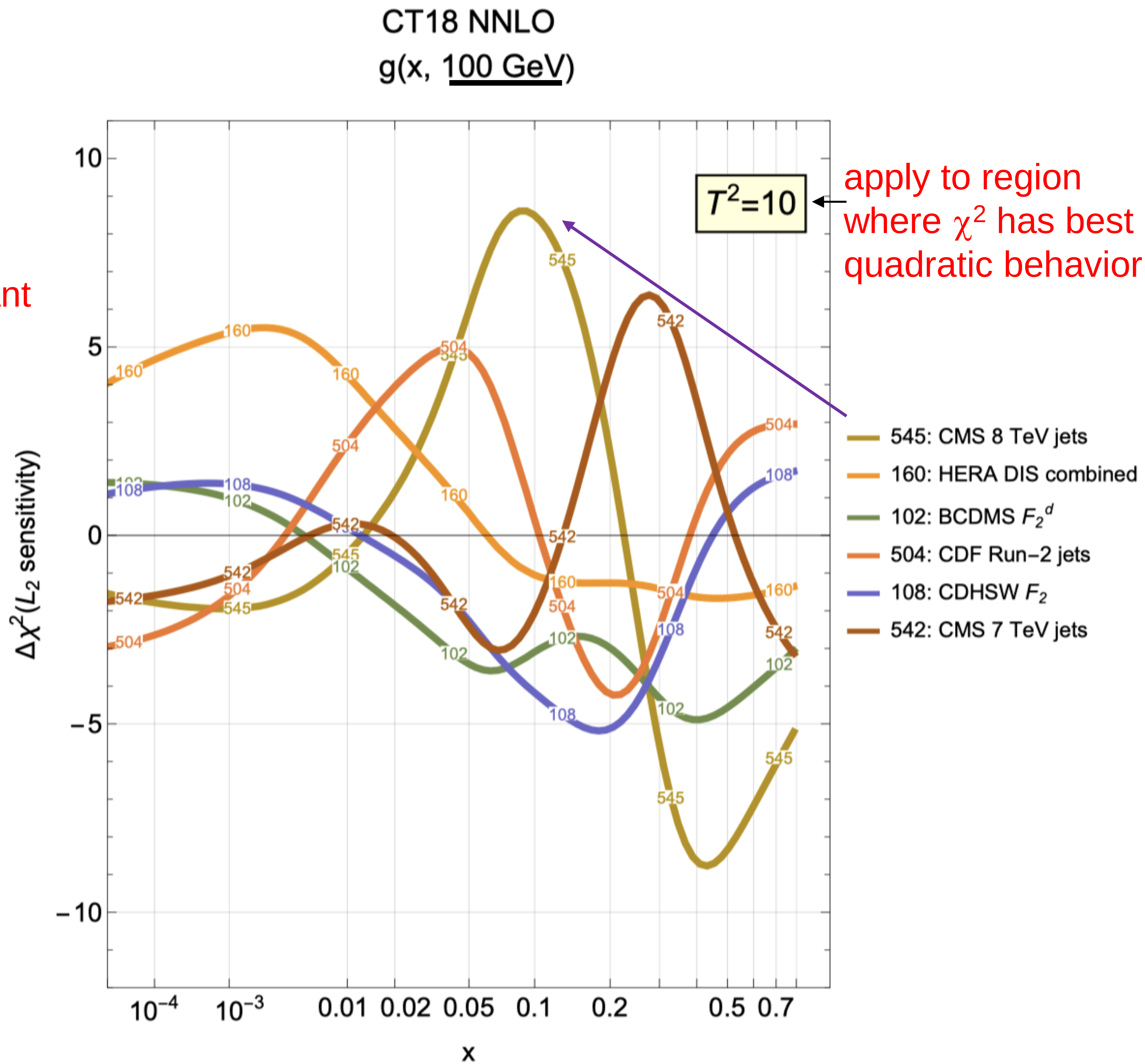

# Can also look at $L_2$ for 2 GeV

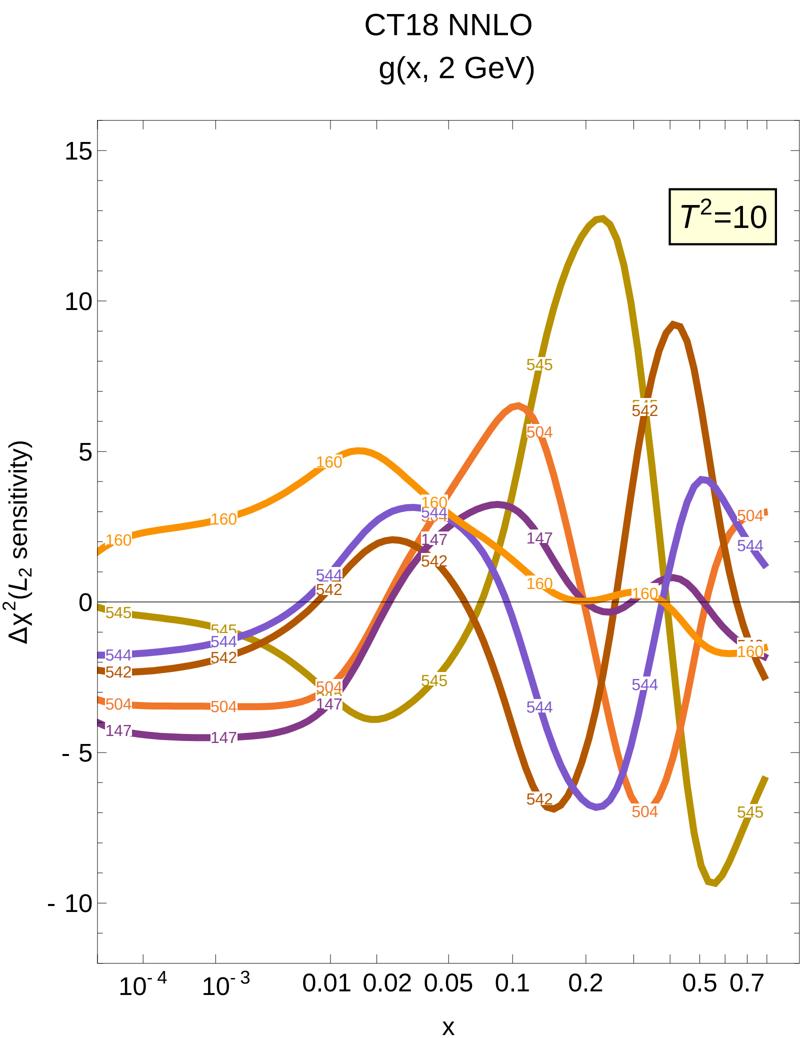


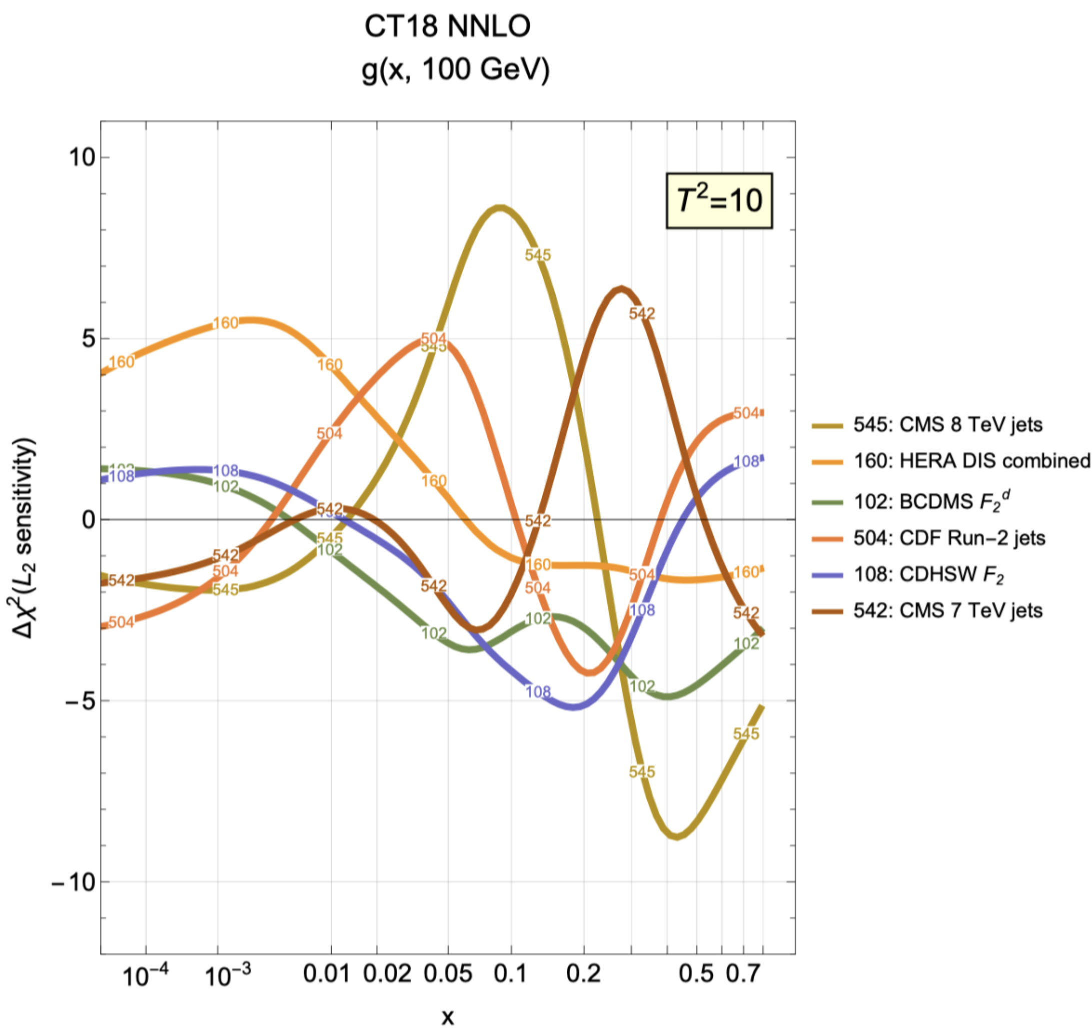

# Lagrange Multplier Scans

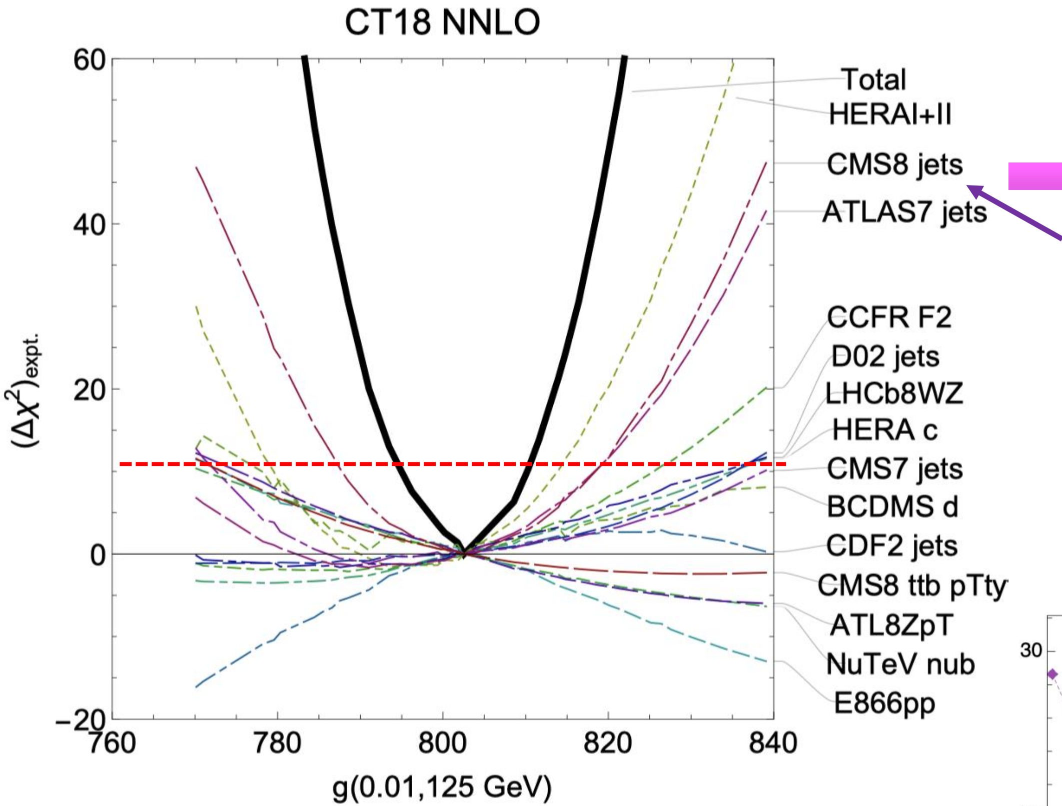


compare to LM scans of the gluon at x=0.01 and x=0.3

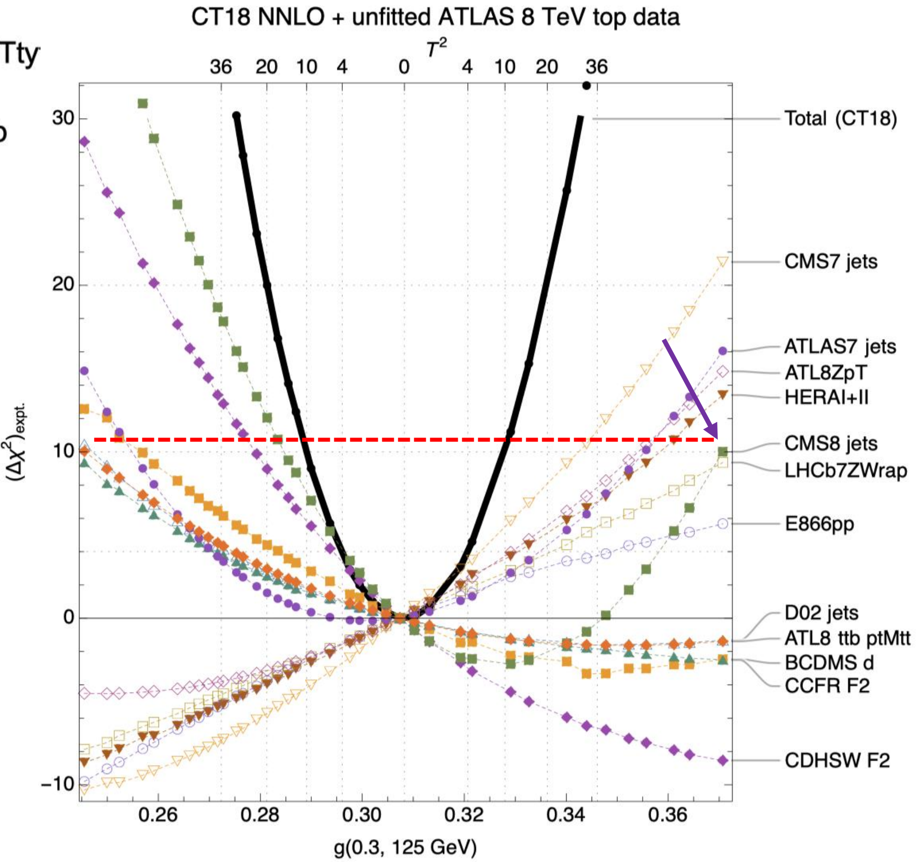

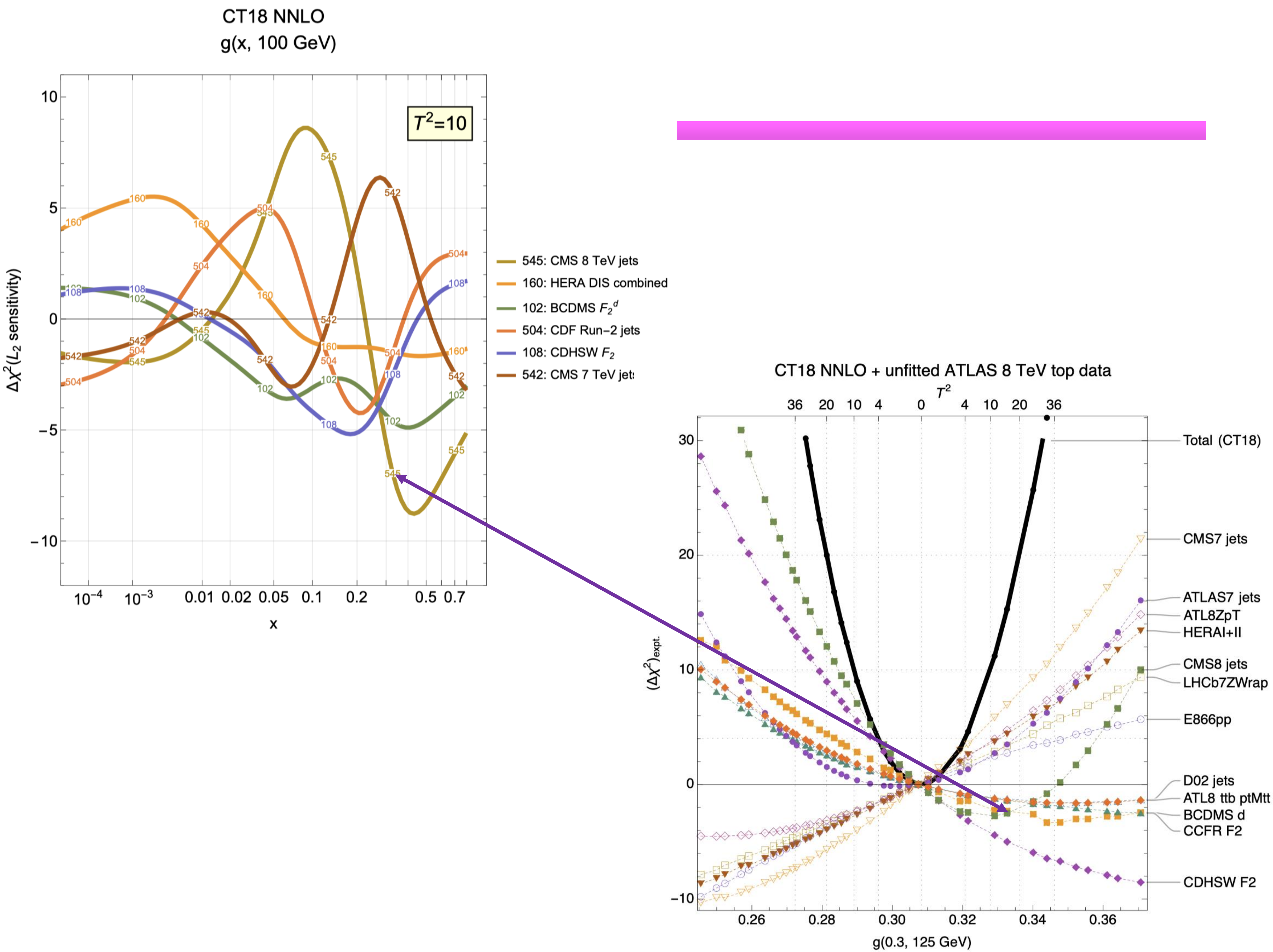
CT18 NNLO
g(x, 100 GeV)
T²=10
Δχ²(L₂ sensitivity)
x
545: CMS 8 TeV jets
160: HERA DIS combined
102: BCDMS F₂ᵈ
504: CDF Run−2 jets
108: CDHSW F₂
542: CMS 7 TeV jets
CT18 NNLO + unfitted ATLAS 8 TeV top data
T²
(Δχ²)expt.
g(0.3, 125 GeV)
Total (CT18)
CMS7 jets
ATLAS7 jets
ATL8ZpT
HERAI+II
CMS8 jets
LHCb7ZWrap
E866pp
D02 jets
ATL8 ttb ptMtt
BCDMS d
CCFR F2
CDHSW F2

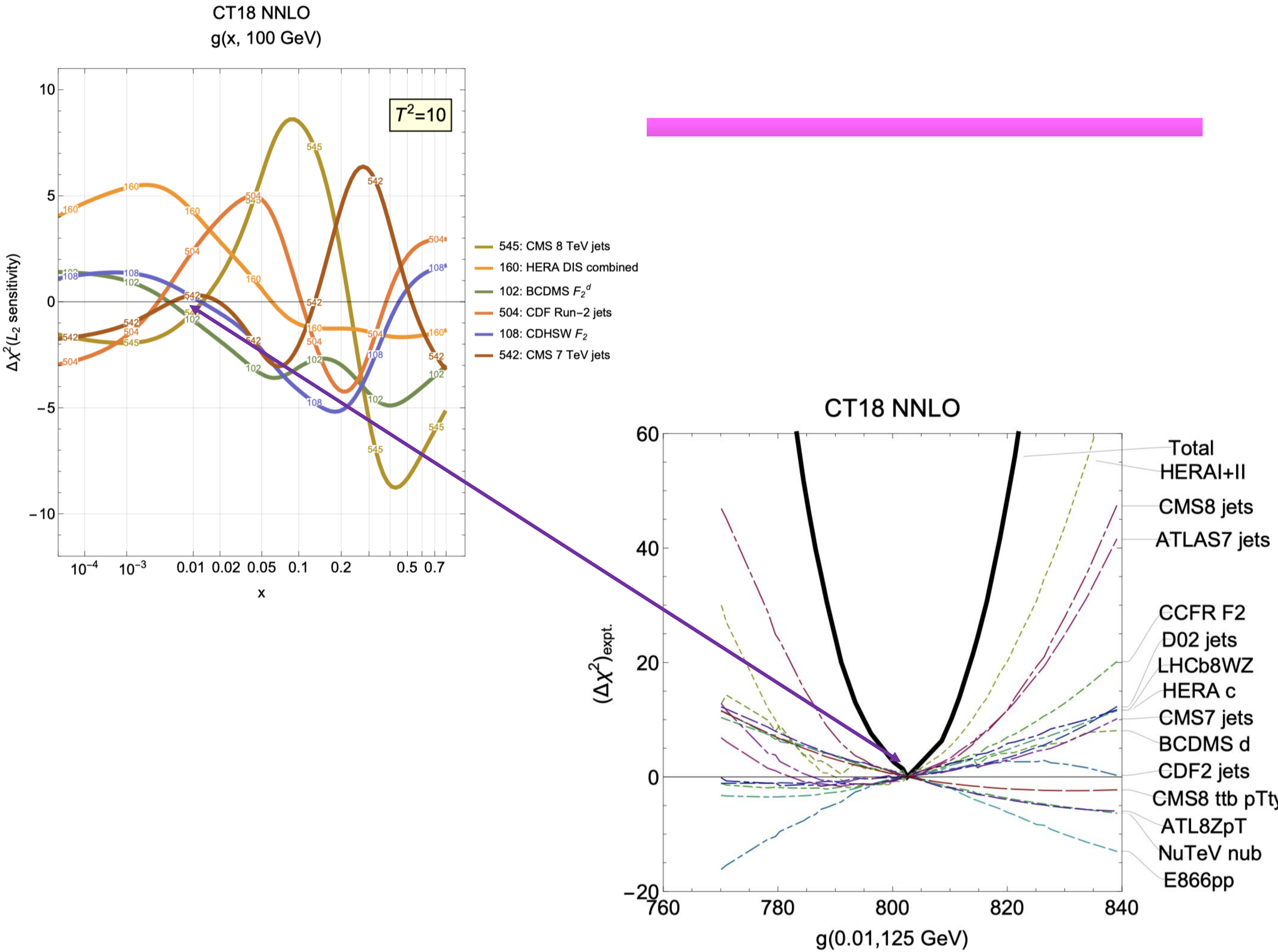
CT18 NNLO
g(x, 100 GeV)
T²=10
Δχ²(L₂ sensitivity)
x
545: CMS 8 TeV jets
160: HERA DIS combined
102: BCDMS F₂ᵈ
504: CDF Run−2 jets
108: CDHSW F₂
542: CMS 7 TeV jets
CT18 NNLO
(Δχ²)expt.
g(0.01,125 GeV)
Total
HERAI+II
CMS8 jets
ATLAS7 jets
CCFR F2
D02 jets
LHCb8WZ
HERA c
CMS7 jets
BCDMS d
CDF2 jets
CMS8 ttb pTty
ATL8ZpT
NuTeV nub
E866pp

TABLE I. Datasets included in the CT18(Z) NNLO global analyses. Here we directly compare the quality of fit found for CT18 NNLO vs CT18Z NNLO on the basis of $\chi^2_E$, $\chi^2_E/N_{pt,E}$, and $S_E$, in which $N_{pt,E}$, $\chi^2_E$ are the number of points and value of $\chi^2$ for experiment $E$ at the global minimum. $S_E$ is the effective Gaussian parameter [38,42,56] quantifying agreement with each experiment. The ATLAS 7 TeV 35 pb$^{-1}$ $W/Z$ dataset, marked by ‡‡, is replaced by the updated one (4.6 fb$^{-1}$) in the CT18A and CT18Z fits. The CDHSW data, labeled by †, are not included in the CT18Z fit. The numbers in parentheses are for the CT18Z NNLO fit.

| Exp. ID# | Experimental dataset | | $N_{pt,E}$ | $\chi^2_E$ | $\chi^2_E/N_{pt,E}$ | $S_E$ |
|---|---|---|---|---|---|---|
| 160 | HERAI + II 1 fb$^{-1}$, H1 and ZEUS NC and CC $e^{\pm}p$ reduced cross sec. comb. | [30] | 1120 | 1408 (1378) | 1.3 (1.2) | 5.7 (5.1) |
| 101 | BCDMS $F_2^p$ | [57] | 337 | 374 (384) | 1.1 (1.1) | 1.4 (1.8) |
| 102 | BCDMS $F_2^d$ | [58] | 250 | 280 (287) | 1.1 (1.1) | 1.3 (1.6) |
| 104 | NMC $F_2^d/F_2^p$ | [59] | 123 | 126 (116) | 1.0 (0.9) | 0.2 (−0.4) |
| 108† | CDHSW $F_2^p$ | [60] | 85 | 85.6 (86.8) | 1.0 (1.0) | 0.1 (0.2) |
| 109† | CDHSW $x_B F_3^p$ | [60] | 96 | 86.5 (85.6) | 0.9 (0.9) | −0.7 (−0.7) |
| 110 | CCFR $F_2^p$ | [61] | 69 | 78.8 (76.0) | 1.1 (1.1) | 0.9 (0.6) |
| 111 | CCFR $x_B F_3^p$ | [62] | 86 | 33.8 (31.4) | 0.4 (0.4) | −5.2 (−5.6) |
| 124 | NuTeV $\nu\mu\mu$ SIDIS | [63] | 38 | 18.5 (30.3) | 0.5 (0.8) | −2.7 (−0.9) |
| 125 | NuTeV $\bar{\nu}\mu\mu$ SIDIS | [63] | 33 | 38.5 (56.7) | 1.2 (1.7) | 0.7 (2.5) |
| 126 | CCFR $\nu\mu\mu$ SIDIS | [64] | 40 | 29.9 (35.0) | 0.7 (0.9) | −1.1 (−0.5) |
| 127 | CCFR $\bar{\nu}\mu\mu$ SIDIS | [64] | 38 | 19.8 (18.7) | 0.5 (0.5) | −2.5 (−2.7) |
| 145 | H1 $\sigma_r^b$ | [65] | 10 | 6.8 (7.0) | 0.7 (0.7) | −0.6 (−0.6) |
| 147 | Combined HERA charm production | [66] | 47 | 58.3 (56.4) | 1.2 (1.2) | 1.1 (1.0) |
| 169 | H1 $F_L$ | [33] | 9 | 17.0 (15.4) | 1.9 (1.7) | 1.7 (1.4) |
| 201 | E605 Drell-Yan process | [67] | 119 | 103.4 (102.4) | 0.9 (0.9) | −1.0 (−1.1) |
| 203 | E866 Drell-Yan process $\sigma_{pd}/(2\sigma_{pp})$ | [68] | 15 | 16.1 (17.9) | 1.1 (1.2) | 0.3 (0.6) |
| 204 | E866 Drell-Yan process $Q^3 d^2\sigma_{pp}/(dQ dx_F)$ | [69] | 184 | 244 (240) | 1.3 (1.3) | 2.9 (2.7) |
| 225 | CDF run-1 lepton $A_{ch}$, $p_{T\ell} > 25$ GeV | [70] | 11 | 9.0 (9.3) | 0.8 (0.8) | −0.3 (−0.2) |
| 227 | CDF run-2 electron $A_{ch}$, $p_{T\ell} > 25$ GeV | [71] | 11 | 13.5 (13.4) | 1.2 (1.2) | 0.6 (0.6) |
| 234 | DØ run-2 muon $A_{ch}$, $p_{T\ell} > 20$ GeV | [72] | 9 | 9.1 (9.0) | 1.0 (1.0) | 0.2 (0.1) |
| 260 | DØ run-2 $Z$ rapidity | [73] | 28 | 16.9 (18.7) | 0.6 (0.7) | −1.7 (−1.3) |
| 261 | CDF run-2 $Z$ rapidity | [74] | 29 | 48.7 (61.1) | 1.7 (2.1) | 2.2 (3.3) |
| 266 | CMS 7 TeV 4.7 fb$^{-1}$, muon $A_{ch}$, $p_{T\ell} > 35$ GeV | [75] | 11 | 7.9 (12.2) | 0.7 (1.1) | −0.6 (0.4) |
| 267 | CMS 7 TeV 840 pb$^{-1}$, electron $A_{ch}$, $p_{T\ell} > 35$ GeV | [76] | 11 | 4.6 (5.5) | 0.4 (0.5) | −1.6 (−1.3) |
| 268‡‡ | ATLAS 7 TeV 35 pb$^{-1}$ $W/Z$ cross sec., $A_{ch}$ | [77] | 41 | 44.4 (50.6) | 1.1 (1.2) | 0.4 (1.1) |
| 281 | DØ run-2 9.7 fb$^{-1}$ electron $A_{ch}$, $p_{T\ell} > 25$ GeV | [78] | 13 | 22.8 (20.5) | 1.8 (1.6) | 1.7 (1.4) |
| 504 | CDF run-2 inclusive jet production | [79] | 72 | 122 (117) | 1.7 (1.6) | 3.5 (3.2) |
| 514 | DØ run-2 inclusive jet production | [80] | 110 | 113.8 (115.2) | 1.0 (1.0) | 0.3 (0.4) |

TABLE II. Like Table I, for newly included LHC measurements. The ATLAS 7 TeV $W/Z$ data (4.6 fb$^{-1}$), labeled by ‡, are included in the CT18A and CT18Z global fits, but not in CT18 and CT18X.

| Exp. ID# | Experimental dataset | | $N_{pt,E}$ | $\chi^2_E$ | $\chi^2_E/N_{pt,E}$ | $S_E$ |
|---|---|---|---|---|---|---|
| 245 | LHCb 7 TeV 1.0 fb$^{-1}$ $W/Z$ forward rapidity cross sec. | [81] | 33 | 53.8 (39.9) | 1.6 (1.2) | 2.2 (0.9) |
| 246 | LHCb 8 TeV 2.0 fb$^{-1}$ $Z \to e^- e^+$ forward rapidity cross sec. | [82] | 17 | 17.7 (18.0) | 1.0 (1.1) | 0.2 (0.3) |
| 248‡ | ATLAS 7 TeV 4.6 fb$^{-1}$, $W/Z$ combined cross sec. | [39] | 34 | 287.3 (88.7) | 8.4 (2.6) | 13.7 (4.8) |
| 249 | CMS 8 TeV 18.8 fb$^{-1}$ muon charge asymmetry $A_{ch}$ | [83] | 11 | 11.4 (12.1) | 1.0 (1.1) | 0.2 (0.4) |
| 250 | LHCb 8 TeV 2.0 fb$^{-1}$ $W/Z$ cross sec. | [84] | 34 | 73.7 (59.4) | 2.1 (1.7) | 3.7 (2.6) |
| 253 | ATLAS 8 TeV 20.3 fb$^{-1}$, $Z$ $p_T$ cross sec. | [85] | 27 | 30.2 (28.3) | 1.1 (1.0) | 0.5 (0.3) |
| 542 | CMS 7 TeV 5 fb$^{-1}$, single incl. jet cross sec., $R = 0.7$ (extended in y) | [86] | 158 | 194.7 (188.6) | 1.2 (1.2) | 2.0 (1.7) |
| 544 | ATLAS 7 TeV 4.5 fb$^{-1}$, single incl. jet cross sec., $R = 0.6$ | [9] | 140 | 202.7 (203.0) | 1.4 (1.5) | 3.3 (3.4) |
| 545 | CMS 8 TeV 19.7 fb$^{-1}$, single incl. jet cross sec., $R = 0.7$, (extended in y) | [87] | 185 | 210.3 (207.6) | 1.1 (1.1) | 1.3 (1.2) |
| 573 | CMS 8 TeV 19.7 fb$^{-1}$, $t\bar{t}$ norm. double-diff. top $p_T$ and $y$ cross sec. | [88] | 16 | 18.9 (19.1) | 1.2 (1.2) | 0.6 (0.6) |
| 580 | ATLAS 8 TeV 20.3 fb$^{-1}$, $t\bar{t}$ $p_T^t$ and $m_{t\bar{t}}$ abs. spectrum | [89] | 15 | 9.4 (10.7) | 0.6 (0.7) | −1.1 (−0.8) |

since first derivative of $\chi^2$ vanishes at the global minimum, the sum of the $L_2$ sensitivities must be zero within uncertainties

$$0 < \sum_E S_{f,L_2} \ll T^2 < \sum_E |S_{f,L_2}|$$

# Examine the impact of each experiment on the different PDFs

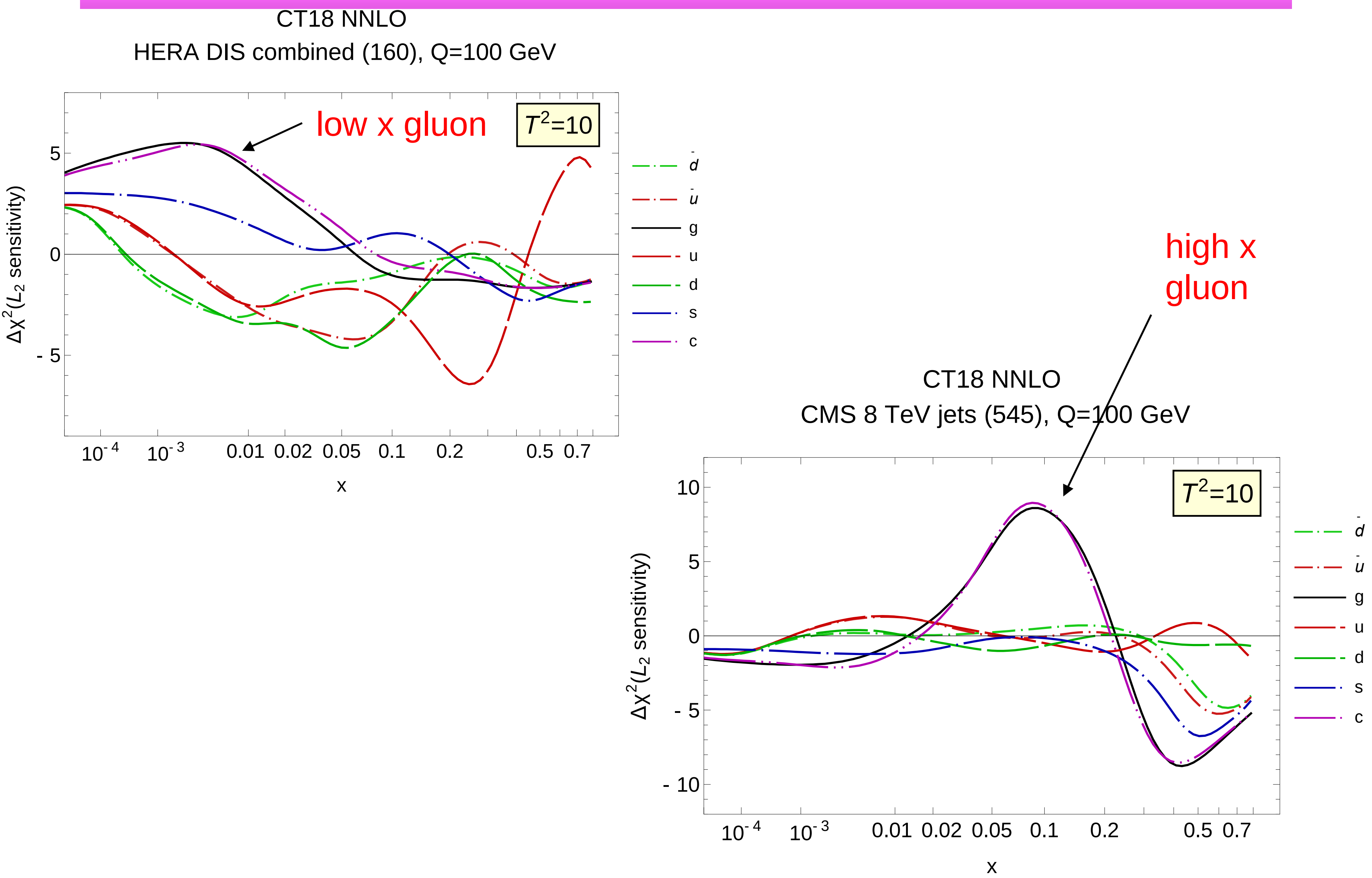

# MSHT20 NNLO gluon

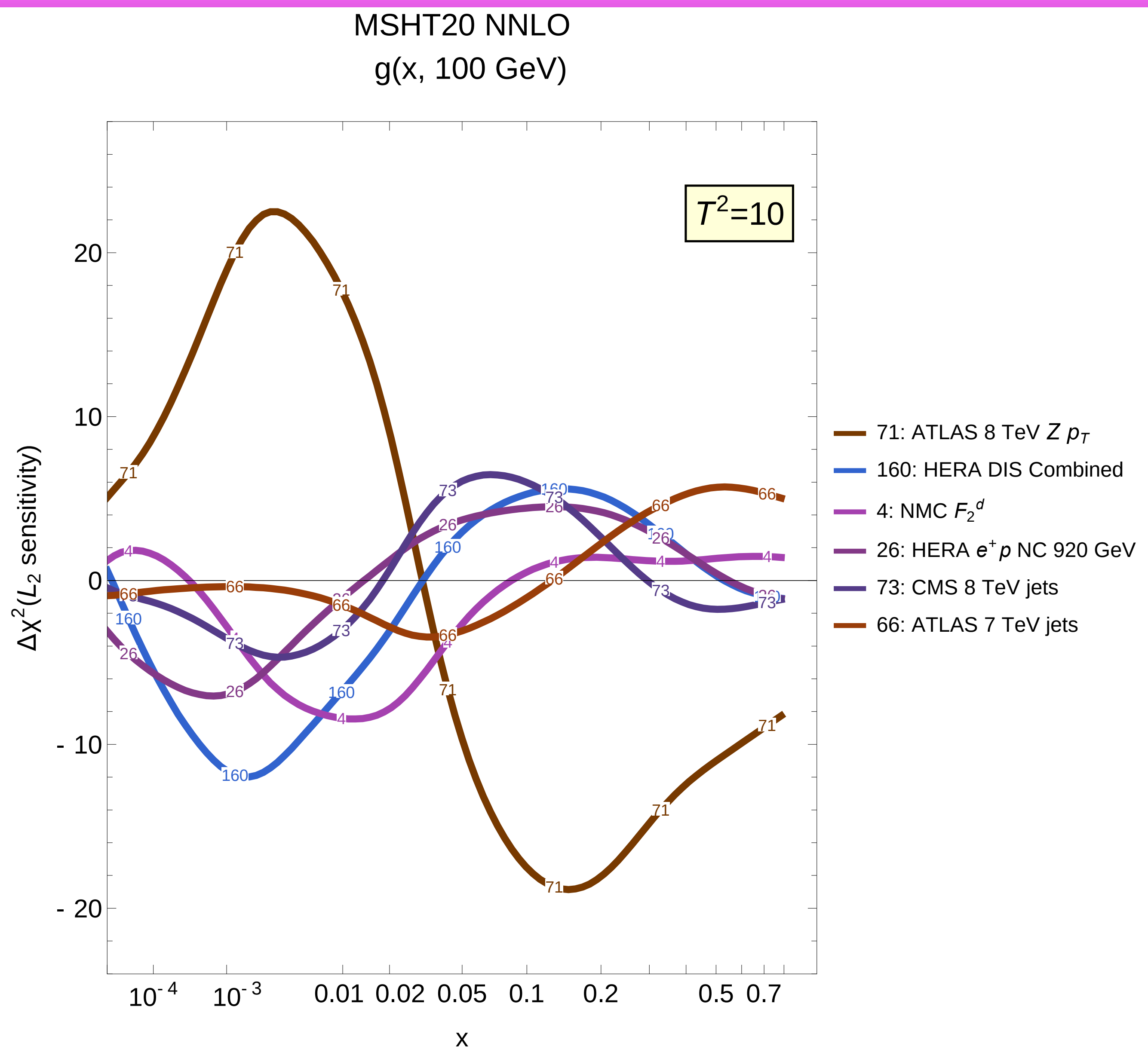

# MSHT20 and CT18

Note importance of ATLAS Z $p_T$ data
(also, Z $p_T$ data poorly fit at NNLO; dynamic tolerance?)

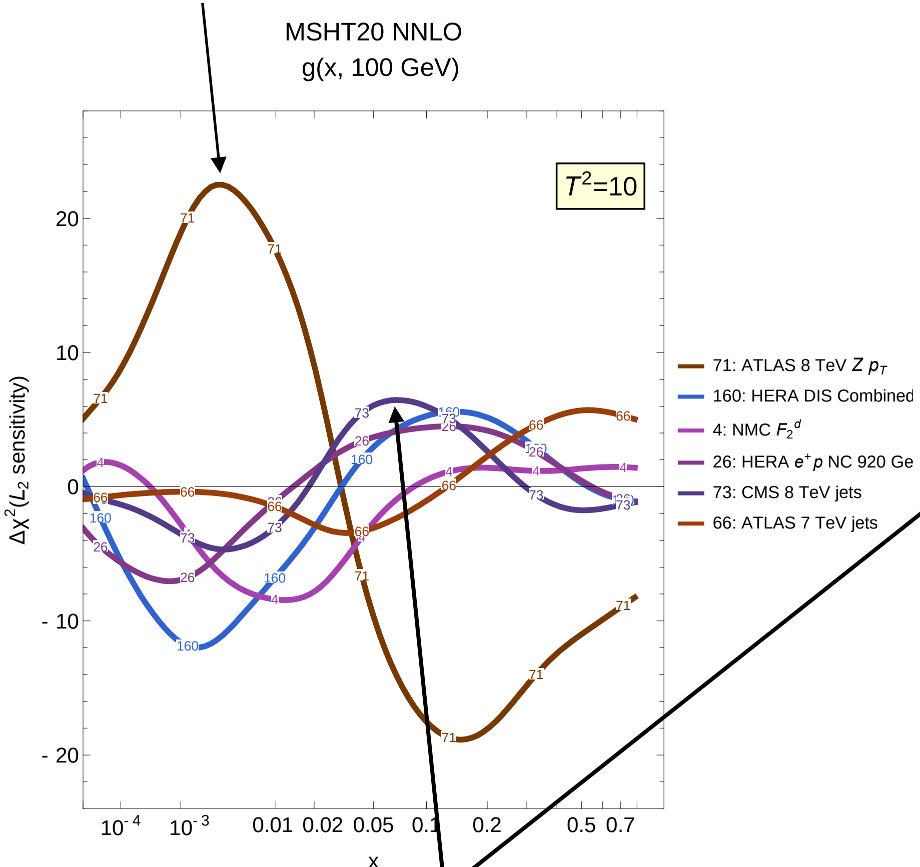


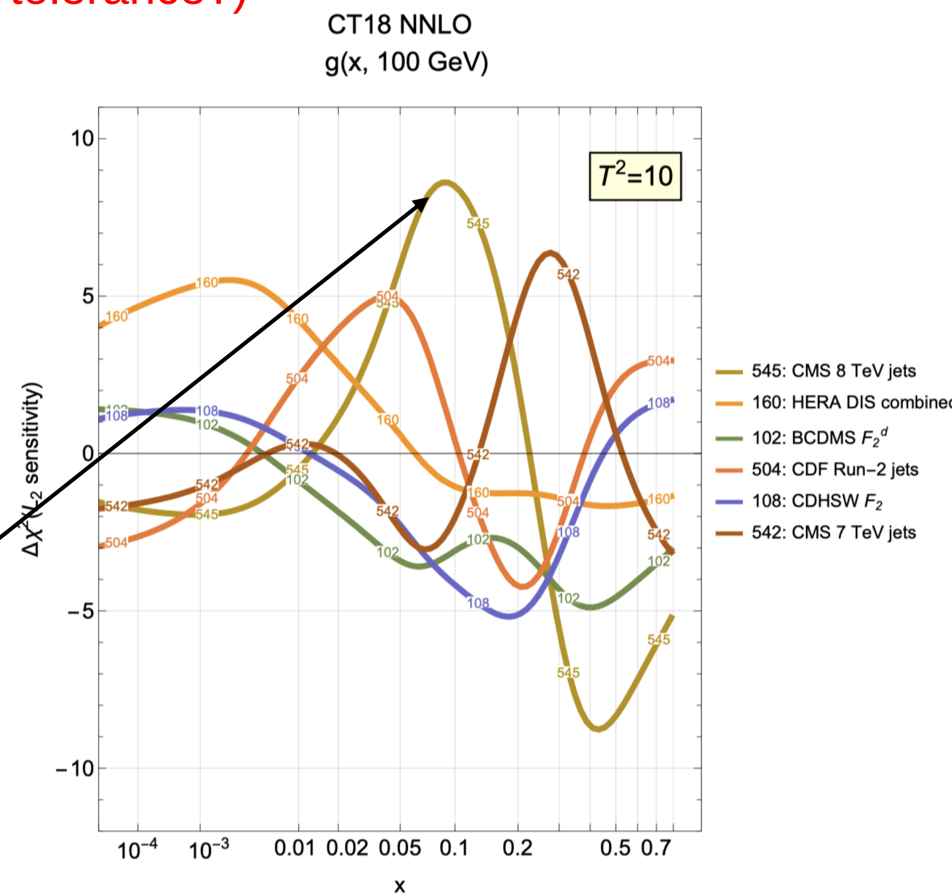


CMS 8 TeV jet data play a similar role as in CT18

ATLAS Z $p_T$ not one of 6 most important experiments (more restrictive kinematic region)

# MSHT20 NNLO and aN3LO

shape of $L_2$ sensitivity similar for two PDFs, but absolute value of Z $p_T$ decreased by almost a factor of 3; significant change in low x gluon

MSHT20 NNLO
g(x, 100 GeV)

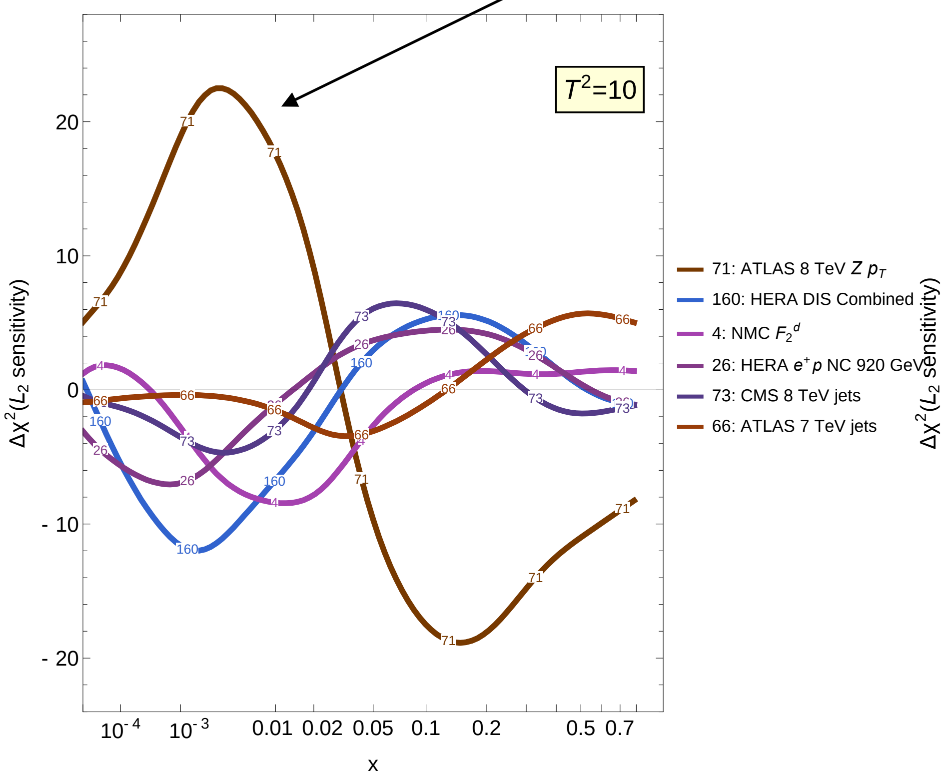


MSHT20 approx. N3LO
g(x, 100 GeV)

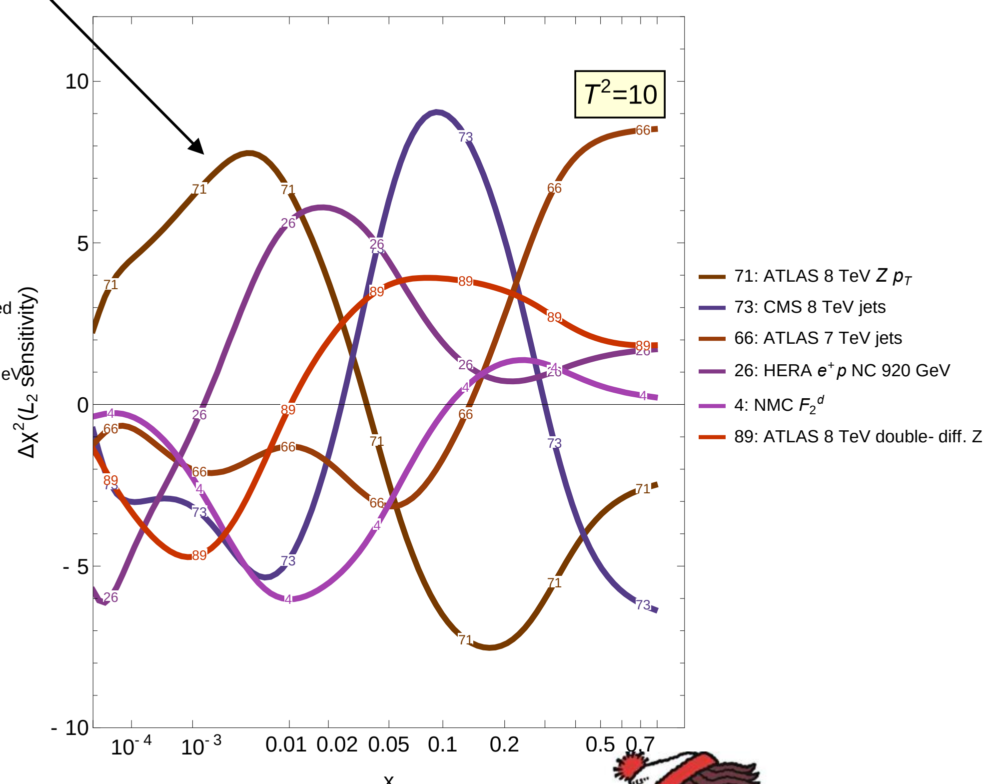


where's expt 160?

# MSHT20 NNLO and aN3LO

at aN3LO, the two experiments now on same side; aN3LO needed for HERA

MSHT20 NNLO
g(x, 100 GeV)

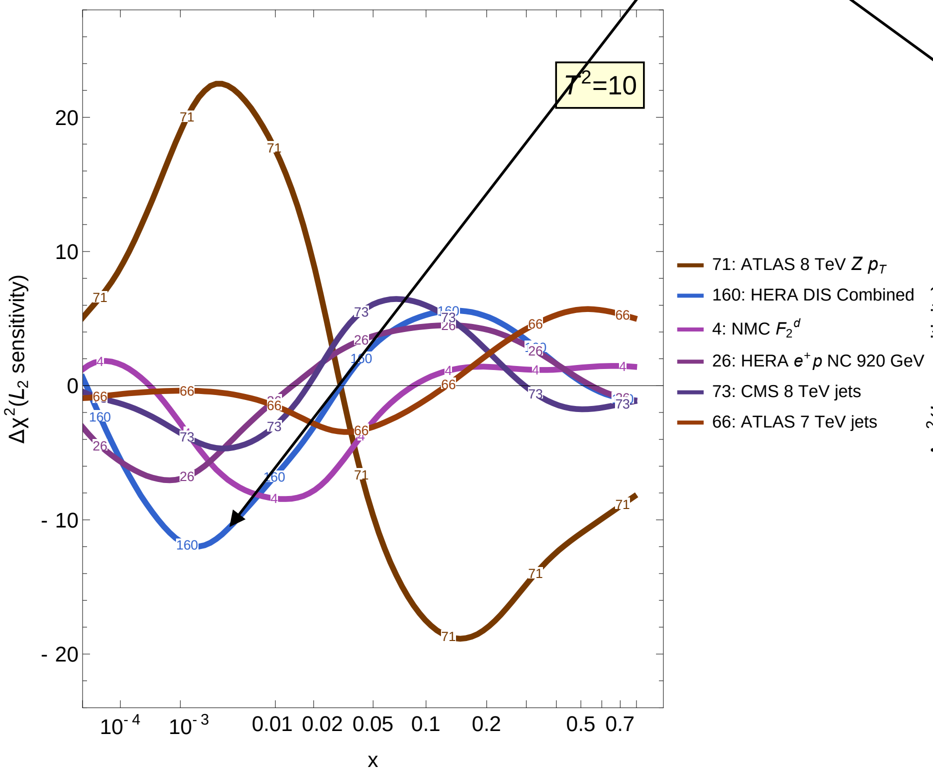


MSHT20 approx. N3LO
g(x, 100 GeV)

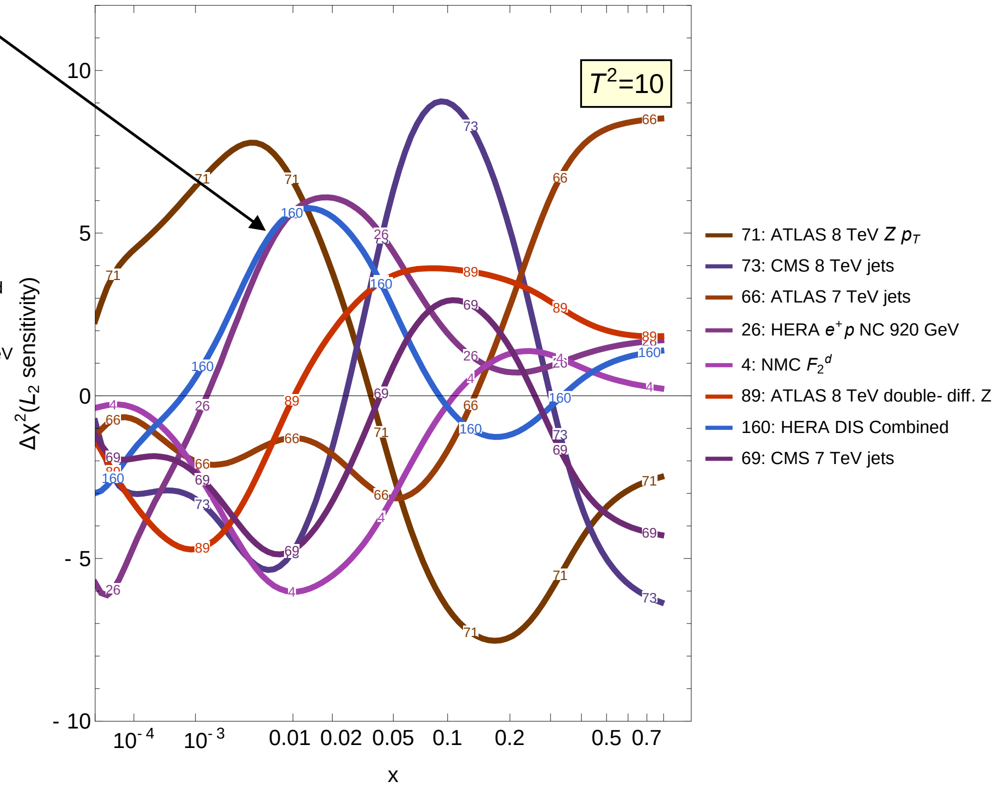


160 fell out of the top 6

# ATLASpdf21

ATLAS PDF fits are based on a more limited set of data, with HERA inclusive as the backbone

series of sequential PDF fits adding W/Z data,ttbar, W/Z+jets, inclusive jets and photon ratio data

full information on correlated systematic sources of uncertainty used (not available to to other PDF fits)

| ID | Data set | $\sqrt{s}$ [TeV] | Luminosity [fb$^{-1}$] | Decay channel | Observables entering the fit |
|---|---|---|---|---|---|
| 160 | HERA inclusive DIS [26] | Varied | Varied | | Reduced cross sections |
| 68 | Inclusive $W, Z/\gamma^*$ [27] | 7 | 4.6 | $e, \mu$ combined | $\eta_\ell$ $(W)$, $y_Z$ $(Z)$ |
| 89 | Inclusive $Z/\gamma^*$ [28] | 8 | 20.2 | $e, \mu$ combined | $\cos\theta^*$ in bins of $y_{\ell\ell}$, $m_{\ell\ell}$ |
| 86 | Inclusive $W$ [29] | 8 | 20.2 | $\mu$ | $\eta_\mu$ |
| 56 | $W^\pm$ + jets [30] | 8 | 20.2 | $e$ | $p_{\mathrm{T}}^W$ |
| | $Z$ + jets [31] | 8 | 20.2 | $e$ | $p_{\mathrm{T}}^{\mathrm{jet}}$ in bins of $\lvert y^{\mathrm{jet}}\rvert$ |
| 7 | $t\bar{t}$ [32, 33] | 8 | 20.2 | lepton + jets, dilepton | $m_{t\bar{t}}$, $p_{\mathrm{T}}^t$, $y_{t\bar{t}}$ |
| 8 | $t\bar{t}$ [34] | 13 | 36 | lepton + jets | $m_{t\bar{t}}$, $p_{\mathrm{T}}^t$, $y_t$, $y_{t\bar{t}}^{\mathrm{b}}$ |
| 9 | Inclusive isolated $\gamma$ [35] | 8, 13 | 20.2, 3.2 | - | $E_{\mathrm{T}}^\gamma$ in bins of $\eta^\gamma$ |
| 10 | Inclusive jets [36–38] | 7, 8, 13 | 4.5, 20.2, 3.2 | - | $p_{\mathrm{T}}^{\mathrm{jet}}$ in bins of $\lvert y^{\mathrm{jet}}\rvert$ |

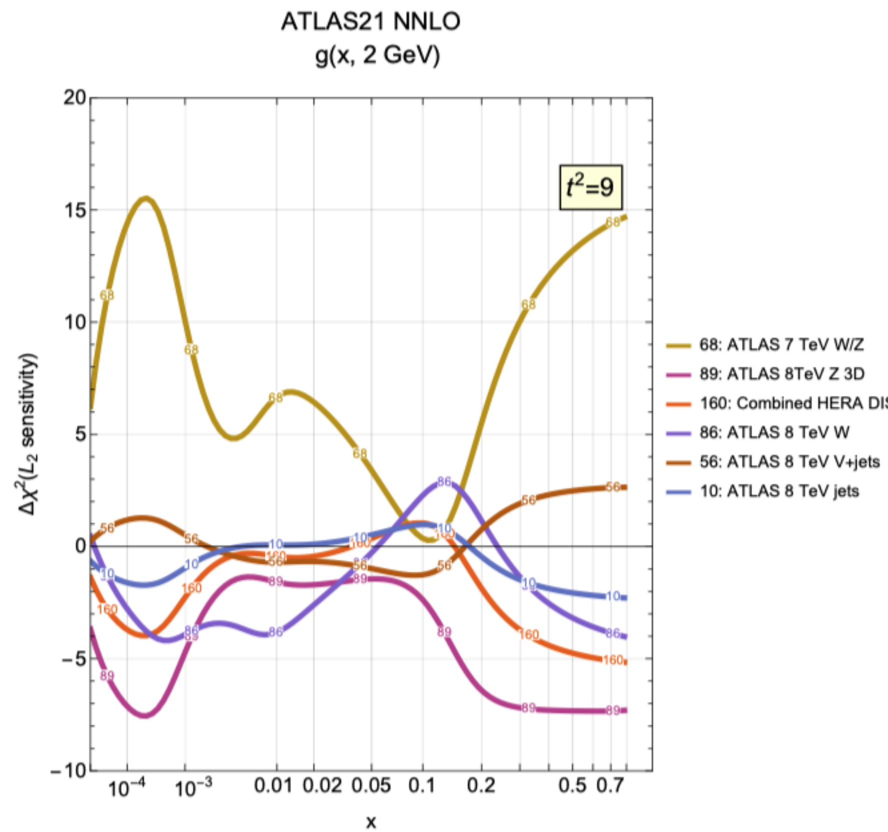

# ATLASpdf21:Impact of addition of W/Z, ttbar data to HERA inclusive

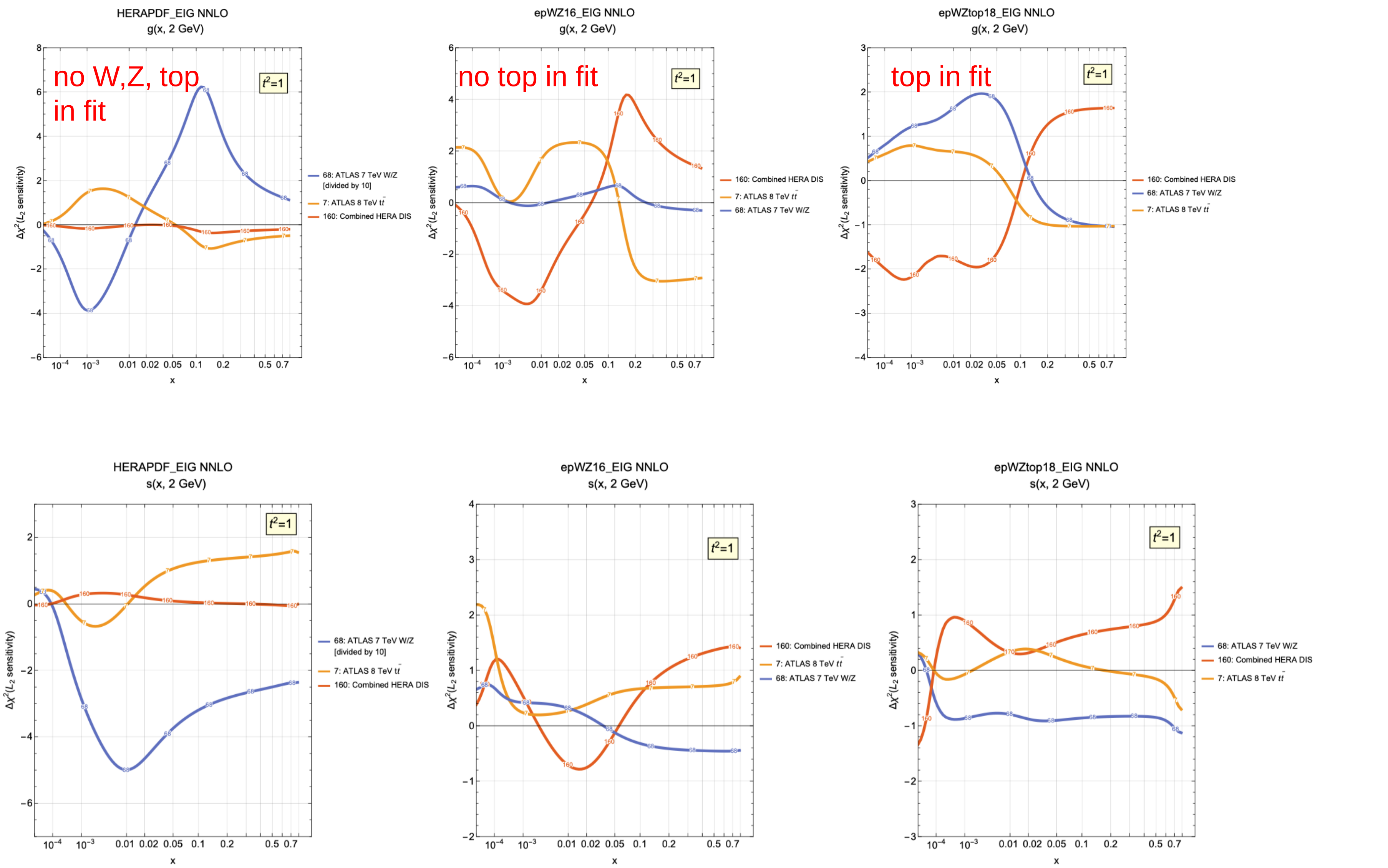

# Reduced fits (PDF4LHC21);arXiV:2203.05506

| Dataset | $N_{\rm pt}$ | $\chi^2/N_{\rm pt}$ | | |
|---|---|---|---|---|
| | | CT18 | MSHT20 | NNPDF3.1 |
| BCDMS $F_2^p$ | $329/163^{\dagger\dagger}/325^{\dagger}$ | 1.06 | 1.00 | 1.21 |
| BCDMS $F_2^d$ | $246/151^{\dagger\dagger}/244^{\dagger}$ | 1.06 | 0.88 | 1.10 |
| NMC $F_2^d/F_2^p$ | $118/117^{\dagger}$ | 0.93 | 0.93 | 0.90 |
| NuTeV dimuon $\nu+\bar{\nu}$ | 38+33 | 0.79 | 0.83 | 1.22 |
| HERAI+II | 1120 | 1.23 | 1.20 | 1.22 |
| E866 $\sigma_{pd}/(2\sigma_{pp})$ | 15 | 1.24 | 0.80 | 0.43 |
| LHCb 7 TeV & 8TeV $W$,$Z$ | 29+30 | 1.15 | 1.17 | 1.44 |
| LHCb 8 TeV $Z\to ee$ | 17 | 1.35 | 1.43 | 1.57 |
| ATLAS 7 TeV $W$,$Z$ (2016) | 34 | 1.96 | 1.79 | 2.33 |
| D0 Z rapidity | 28 | 0.56 | 0.58 | 0.62 |
| CMS 7 TeV electron $A_{\rm ch}$ | 11 | 1.47 | 1.52 | 0.76 |
| ATLAS 7 TeV $W$,$Z$(2011) | 30 | 1.03 | 0.93 | 1.01 |
| CMS 8TeV incl. jet | $185/174^{\dagger\dagger}$ | 1.03 | 1.39 | 1.30 |
| Total $N_{\rm pt}$ | — | 2263 | 1991 | 2256 |
| Total $\chi^2/N_{\rm pt}$ | — | 1.14 | 1.15 | 1.20 |

fitting CT18', MSHT20' and NNPDF3.1' to a common data set, as prelude to the PDF4LHC21 combination

**Table 3.3.** Same as Table 3.2, now displaying the results obtained after each group has carried out the corresponding fits to this reduced dataset. That is, the input PDF is now the best-fit value obtained for each group to the reduced dataset rather than the common PDF4LHC15 PDF input used in Table 3.2. $^{\dagger\dagger}$MSHT $^{\dagger}$NNPDF.

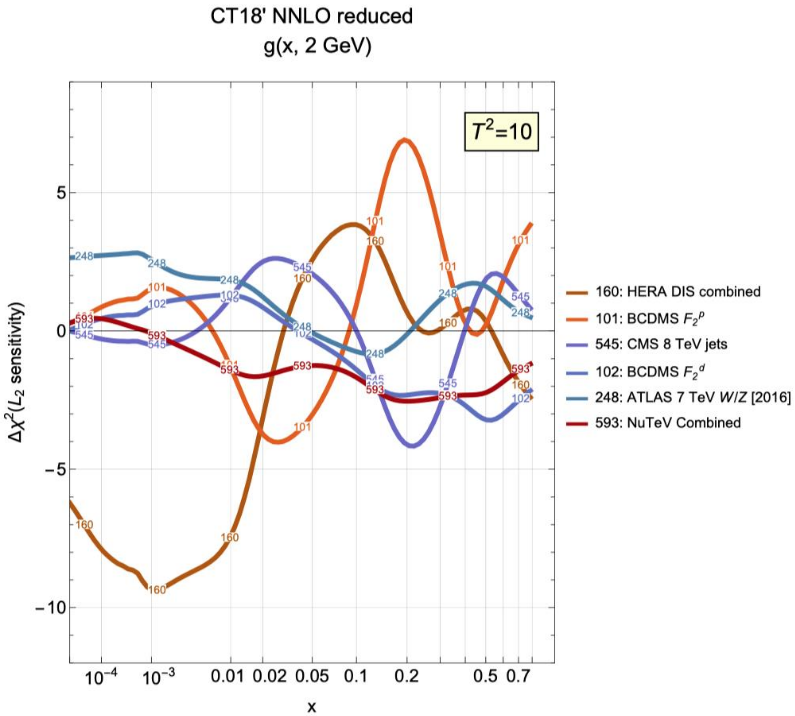


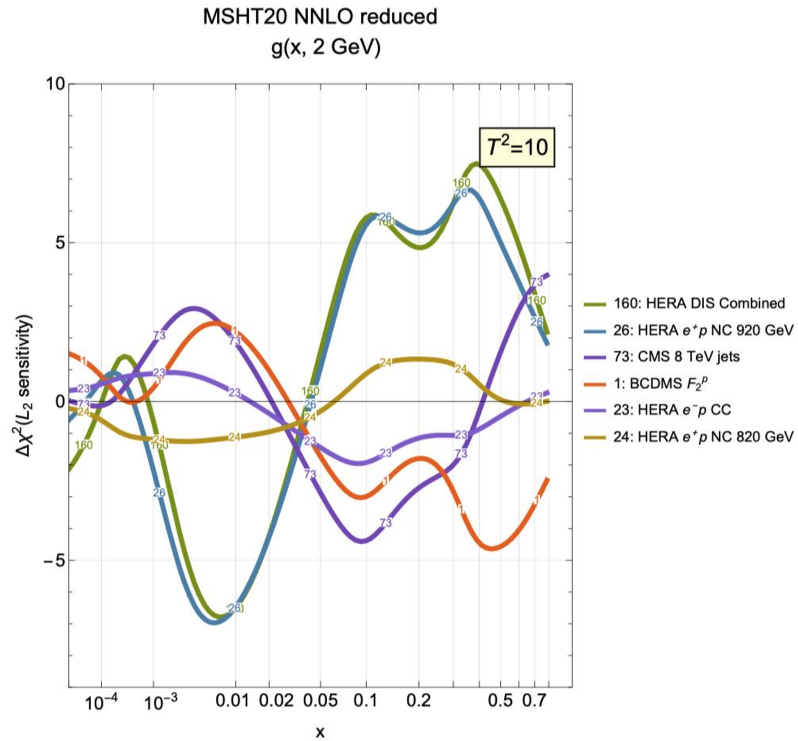


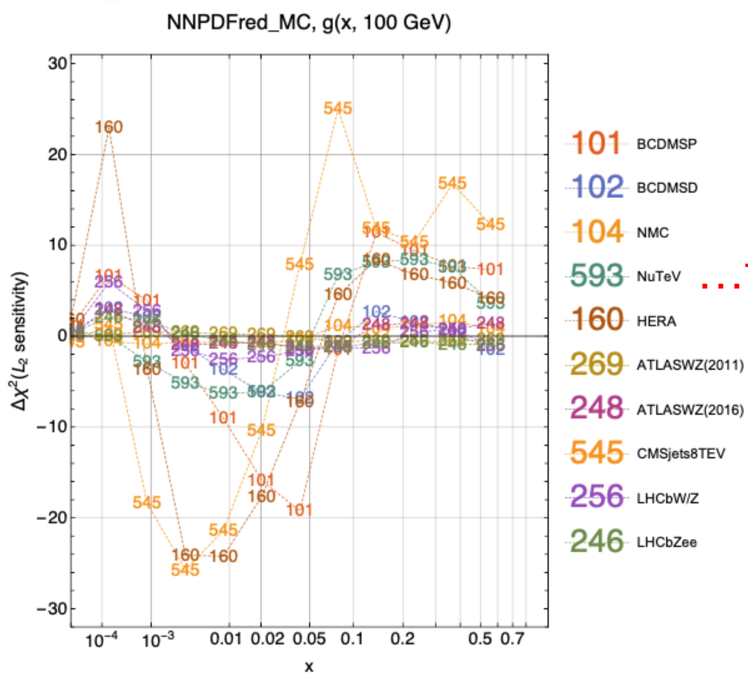


…from PDF4LHC21 paper

# Summary

- $L_2$ sensitivity is a useful variable to understand what is happening/has happened inside a PDF fit, any tensions that may exist between data sets, and how the fit may be improved in the future
- Paper should  be coming out shortly
- Meanwhile, two websites can be used to explore $L_2$ sensitivity for CT18, MSHT20 (NNLO and aN3LO) and ATLASpdf21
  - https://www.physics.smu.edu/nadolsky/work/pdf4lhc21/L2sens/index2.html
  - https://www.physics.smu.edu/nadolsky/work/pdf4lhc21/L2sens/index3.html


You know, it's very strange
I have been in the Remove Trump business so long, now that it's over, I don't know what to do with the rest of my life
Have you ever considered using $L_2$ sensitivity?
[redacted]

# Reduced fits

Reasonable agreement for the most part.

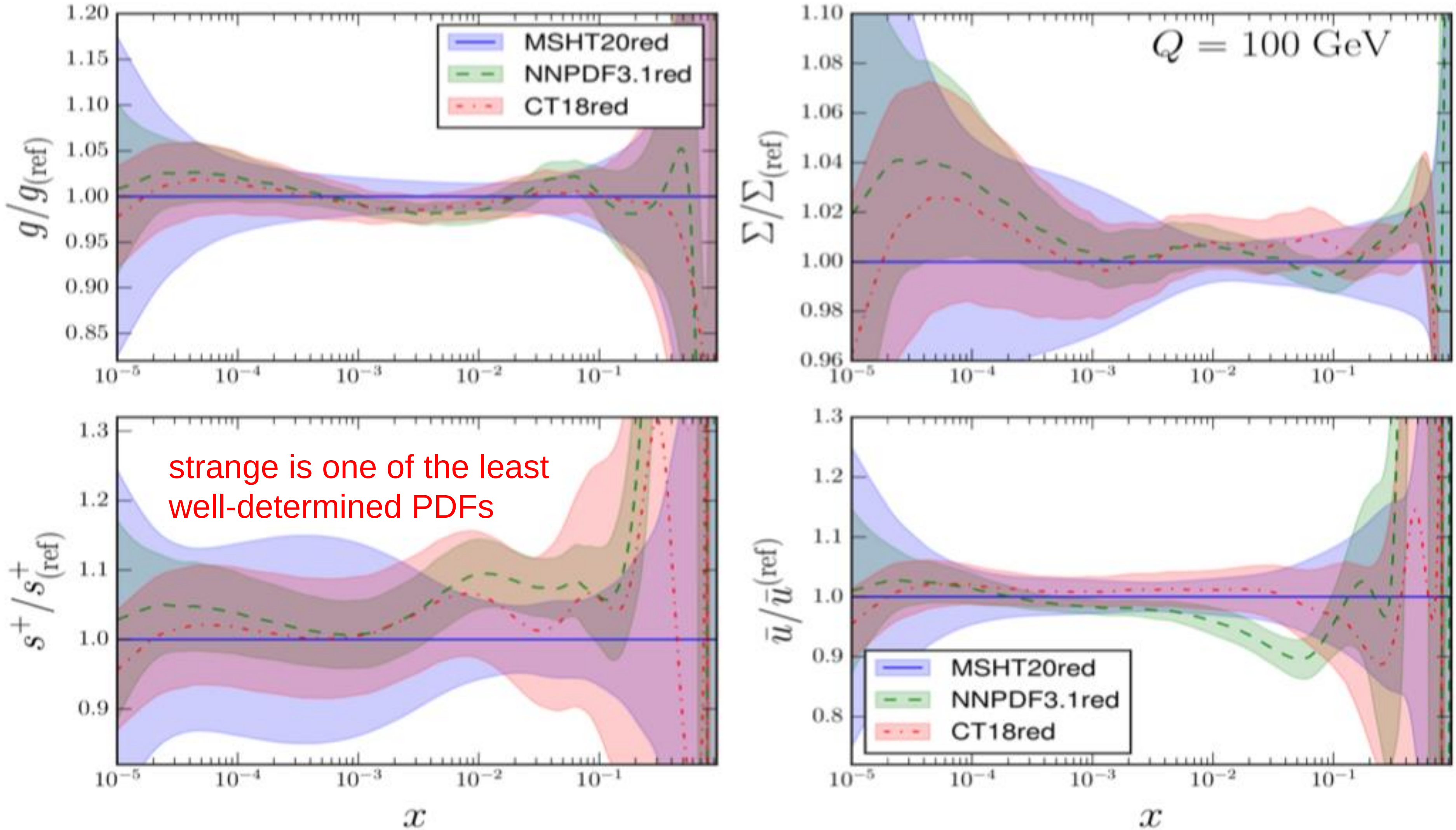

# Uncertainties

Uncertainties increased with respect to full global fits

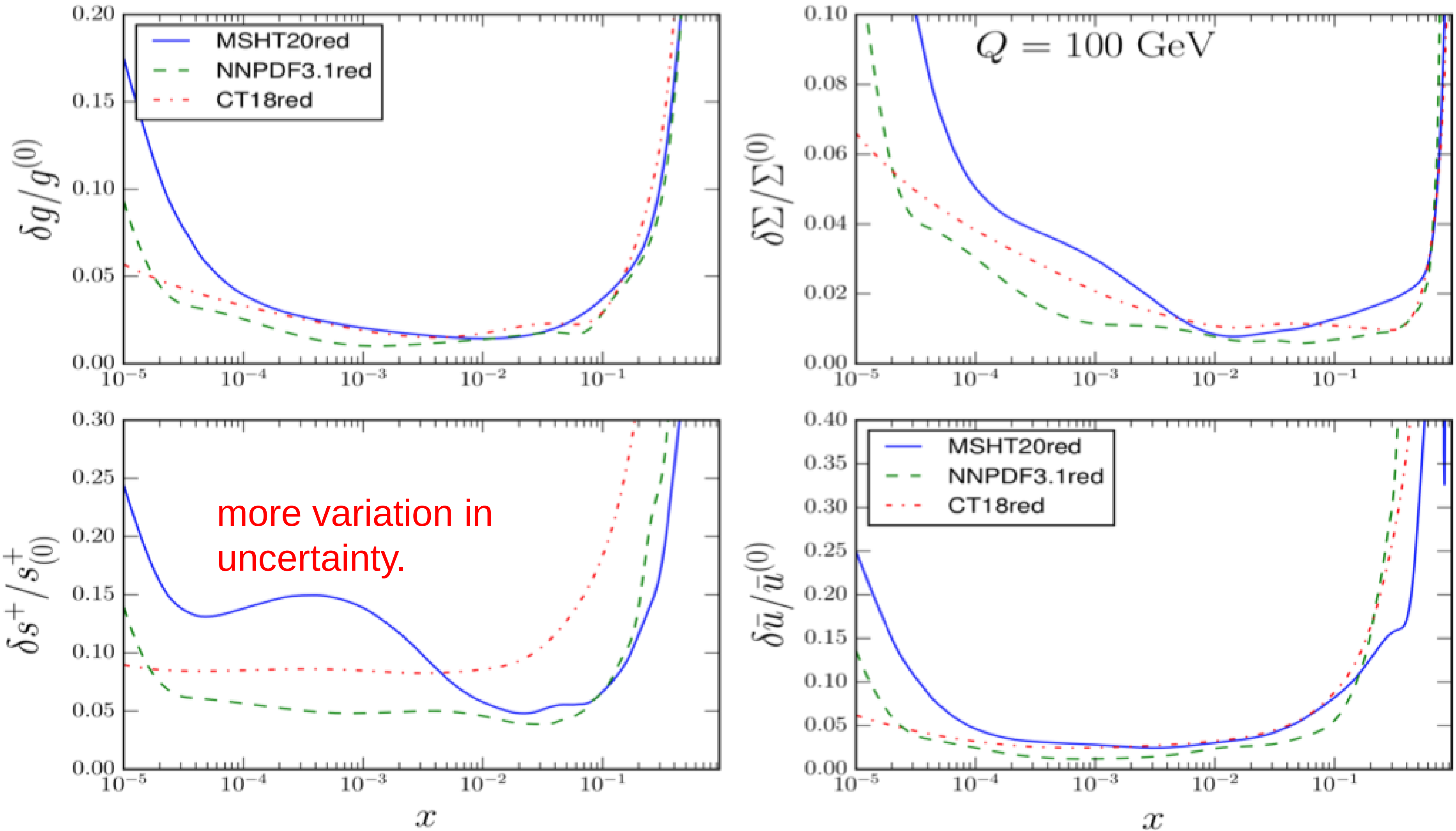

# PDF luminosities